

Received: 2015.12.28
Accepted: 2016.01.25
Published: 2016.09.23

miR-483 is Down-Regulated in Polycystic Ovarian Syndrome and Inhibits KGN Cell Proliferation via Targeting Insulin-Like Growth Factor 1 (IGF1)

Authors' Contribution:
Study Design A
Data Collection B
Statistical Analysis C
Data Interpretation D
Manuscript Preparation E
Literature Search F
Funds Collection G

BCDEF **Yungai Xiang**
BCDF **Yuxia Song**
BCD **Yan Li**
BDF **Dongmei Zhao**
DF **Liyang Ma**
ACE **Li Tan**

Department of Reproductive Medicine, The Second Affiliated Hospital of Zhengzhou University, Zhengzhou, Henan, P.R. China

Corresponding Author: Li Tan, e-mail: tanli37558@126.com
Source of support: Departmental sources

Background: Polycystic ovarian syndrome (PCOS) is a common metabolic disorder in premenopausal woman, characterized by hyperandrogenism, oligoanovulation, and insulin resistance. microRNAs play pivotal roles in regulating key factors of PCOS. However, relevant research remains limited. This study aimed to reveal the role and potential mechanism of miR-483 in PCOS.


Material/Methods: PCOS patients (n=20) were recruited for detecting miR-483 expression in lesion and normal ovary cortex. Human granulosa-like tumor cell line KGN was used to alter miR-483 expression by cell transfection. Cell viability and proliferation were analyzed by MTT assay and colony formation assay, and cell cycle was detected by flow cytometry. Interaction between miR-483 and IGF1 was verified by luciferase reporter assay. KGN cells were further treated by insulin to investigate the relationship between miR-483 and insulin.

Results: miR-483 was significantly down-regulated in lesion ovary cortex from PCOS patients ($P < 0.001$). In KGN cells, overexpression of miR-483 inhibited cell viability and proliferation, and induced cell cycle arrest. miR-483 also inhibited CCNB1, CCND1, and CDK2. miR-483 sponge induced the opposite effects. miR-483 directly targeted IGF1 3'UTR, and IGF1 promoted KGN cell proliferation and reversed miR-483-inhibited cell viability. Insulin treatment in KGN cells inhibited miR-483, and promoted IGF1 and cell proliferation.

Conclusions: These results suggest that miR-483 is a PCOS suppressor inhibiting cell proliferation, possibly via targeting IGF1, and that it is involved in insulin-induced cell proliferation. miR-483 is a potential alternative for diagnosing and treating PCOS.

MeSH Keywords: **Cell Cycle Checkpoints • Cell Proliferation • MicroRNAs • Polycystic Ovary Syndrome • Somatomedins**

Full-text PDF: <http://www.medscimonit.com/abstract/index/idArt/897301>

 3498  1  5  35



Background

Polycystic ovarian syndrome (PCOS) is a set of metabolic and reproductive disorders associated with imbalance in female hormones. It is quite common worldwide, with an approximate incidence of 5% to 10% in females of reproductive age [1]. PCOS patients are usually diagnosed by symptoms like oligoanovulation, high androgen levels, and sclerocystic ovaries, showing irregular menstruation, amenorrhoea, acne, and even difficulty becoming pregnant, which have made PCOS one of the leading causes of infertility [2,3]. To remove the fertility obstacles of PCOS patients, the proper pharmacological induction should be combined with intensive lifestyle intervention such as body weight control [4].

Multiple immature follicles can be detected by ultrasound examination of PCOS. These follicles are generated from disturbed follicle development due to ovarian dysfunction [5], decreased follicle stimulating hormone (FSH) levels, and increased luteinizing hormone (LH) levels [6]. Hyperandrogenism has been considered a vital feature of PCOS [7]. Typically, PCOS patients possess excessive amounts of androgens secreted by the ovaries [8] and elevated androgen receptors in endometrium [9], and a high insulin level may induce excess androgen synthesis [10]. It is reported that the body fat in PCOS patients is more prone to suppress insulin sensitivity, which means a requirement of higher amount of insulin to meet the needs of metabolism [11,12]. Insulin-like growth factor 1 (IGF1) is expressed at higher levels in patients with PCOS and increased insulin resistance [13,14], and the combination of high growth hormone and IGF1 levels contributes to elevated LH and the consequent hyperandrogenism in PCOS patients [15].

microRNAs are noncoding RNA molecules encoded by endogenous genomic sequences, and have been revealed as powerful tools of regulating gene expression in recent decades. microRNAs are reported to be involved in the pathological progression of many diseases, including PCOS, thus becoming promising biomarkers and targets for PCOS diagnosis and treatment. Elevated circulating miR-93 exerts promotive functions in ovarian granulosa cell proliferation, so it may serve as a biomarker for diagnosing PCOS [16,17]. miR-93 is also overexpressed in adipose tissue of PCOS patients and women with insulin resistance [18]. However, few other miRNAs have been reported in the regulation of PCOS.

miR-483 expression is reported to be decreased in cumulus cells of PCOS patients [19], but its role in PCOS is unclear. This study aimed to reveal the roles of miR-483 in PCOS and its potential regulatory mechanism. We analyzed miR-483 expression in lesion and normal ovary cortex of 20 PCOS patients, and altered its levels in human granulosa-like tumor cell line KGN to investigate changes in cell proliferation. IGF1 was confirmed

to be a target for miR-483 in the regulation of KGN cell proliferation. We also found the modulation of miR-483 and IGF1 by insulin. These findings might provide more information on microRNAs and their regulatory roles in PCOS.

Material and Methods

Tissue sampling

The lesion and normal ovarian cortex tissue samples were collected from 20 female patients diagnosed with PCOS and hospitalized from December 2013 to November 2014. The diagnosis of PCOS was based on the *Diagnosis Criteria for PCOS* (Chinese Medical Association, 2011); patients showed the presence of oligo- or anovulation and ultrasound image of polycystic ovaries. Patients with Cushing's syndrome, thyroid dysfunction, late-onset congenital adrenal hyperplasia, and other systemic diseases were excluded from this study. The sampling for PCOS was performed during laparoscopic ovary biopsy [20] and patients were informed before the sampling procedure. None of these patients were pregnant or lactating; none had diabetes, hypertension, or psychiatric disorders; and none were taking oral contraceptive, cholesterol, or antihypertension medications. Briefly, the patients were anesthetized, the abdomino-centesis was performed by trocars, and laparoscopes (diameter=3.3 mm) were inserted. The ovarian cortex tissue samples were collected by biopsy forceps at multiple sites of bilateral ovaries. The tissue samples were quick-frozen in liquid nitrogen and stored at -80°C for miRNA extraction.

Women (n=20) with normal menstruation who underwent laparoscopic sterilization, hysterectomy for benign conditions or diagnostic laparoscopy for pelvic pain were also recruited as the control group for endocrine tests. They accepted endocrine tests and other routine checks and the results are listed in Table 1. Patients with body mass index (BMI) ≥ 25.0 kg/m² were considered overweight. Testosterone ≥ 0.75 ng/mL was considered to be hyperandrogenemia, and insulin ≥ 18.0 $\mu\text{U}/\text{mL}$ was considered to be hyperinsulinism.

Cell culture

Human granulosa-like tumor cell line KGN possessed the physiological characteristics of ovarian cells and was the main cell type producing androgen in the ovaries, so it was used in this study to reveal roles of miR-483. KGN cells (Suer, Shanghai, China) were cultured in Dulbecco's Modified Eagle Medium (DMEM)/F-12 medium (Gibco, Carlsbad, CA) supplemented with 10% fetal bovine serum (FBS, Gibco), 100 U/mL penicillin G, and 0.1 mg/mL streptomycin sulfate (Invitrogen, Carlsbad, CA). The cells were cultured in a humidified atmosphere with 5% CO₂ at 37°C.

Table 1. Diagnosis of patients with or without PCOS.

Variable	Control (n=20)	PCOS (n=20)	P value
AGE (yr)	28.2±3.7	27.3±2.5	NS
BMI (kg/m ²)	22.0±2.5	26.2±3.7	0.027
Normal weight (n)	11	7	0.002
Overweight (n)	9	13	
FSH (mIU/mL)	8.9±0.7	7.9±0.8	0.340
LH (mIU/mL)	6.7±0.7	12.5±1.7	0.004
PRL (ng/mL)	13.7±1.9	35.5±6.1	0.003
E ₂ (pg/mL)	33.5±2.0	68.9±4.0	<0.0001
Glu (mmol/mL)	4.7±1.3	5.9±1.5	0.021
T (ng/mL)	0.38±0.16	0.89±0.25	0.019
Hyperandrogenism (n)	2	12	0.001
Normal androgen level (n)	18	8	
INS (μU/mL)	12.3±1.9	18.6±2.4	0.029
Hyperinsulinism (n)	1	9	0.004
Normal insulinism (n)	19	11	

Measured data are represented as the mean ± SEM. yr – year; BMI – body mass index; FSH – follicle-stimulating hormone; LH – luteinizing hormone; PRL – prolactin; E₂ – estradiol; Glu – glucose. T – testosterone; INS – insulin; IU – international unit; NS – not significant.

Insulin treatment

Insulin treatment was performed to investigate the involvement of miR-483 in the influence of insulin on KGN cells. The cells were divided into 4 groups, seeded in 6-well plates (2×10⁵ cells/well) and treated with recombinant human insulin (Sigma-Aldrich, Shanghai, China) to the final concentration of 0, 1, 10, and 100 ng/mL. After being treated for 48 h, the cells of each group were collected for qRT-PCR, cell viability assay, and colony formation assay.

Cell transfection

The vectors expressing pre-miR-483 and miR-483 sponge were constructed by QuantoBio (Beijing, China) to overexpress and inhibit miR-483. *IGF1*-specific siRNA (RiboBio, Guangzhou, China) and the overexpression vector constructed using the coding sequence of *IGF1* (GenBank No. NM_001111283) and pcDNA3.1 (Thermo Scientific, Carlsbad, CA) were used to alter IGF1 expression. The cells were seeded in 6-well plates (2×10⁵ cells/well) 1 day before transfection to reach the confluency of 90%, and then the medium was replaced by serum- and antibiotic-free medium, after which the transfection procedures were performed by Lipofectamine 2000 (Invitrogen) using 4.0 μg of vectors, according to the manufacturer's instructions. The corresponding blank vectors were transfected as controls. At 48 h after transfection, the cells were collected for the following assays.

Luciferase reporter assay

In order to analyze the direct regulation of *IGF1* by miR-483, we mutated 5 bases in the binding site of miR-483 in *IGF1* 3'UTR using QuikChange Multi Site-Directed Mutagenesis Kit (Agilent Technologies, Santa Clara, CA). The wildtype and mutant *IGF1* 3'UTR were separately cloned into pGL3-promoter luciferase vector (Promega, Madison, WI), and then the vectors were transfected into KGN cells with altered miR-483 expression and the corresponding control groups according to the procedures mentioned above. Luciferase activity was measured by Dual-Luciferase Reporter Assay and GloMax (Promega), with Renilla luciferase reporter plasmid pRL-RSV (Promega) as an internal reference.

Cell viability assay

Cell viability was measured with the MTT method at 24, 48, and 72 h after transfection. The cells in logarithmic phase were seeded in 96-well plates (1×10⁴ cells/well) and cultured overnight in a humidified atmosphere with 5% CO₂ at 37°C. For cells treated by insulin, the cells were first seeded in 96-well plates with medium containing 0 or 100 ng/mL insulin and cultured for 24, 48, or 72 h, and then the following procedures were performed. Briefly, 20 μL of MTT (5 mg/mL in phosphate-buffered saline (PBS), pH 7.4, Sigma-Aldrich) was added to each well for 4-h incubation, after which the medium was removed

and 150 μ L of dimethylsulfoxide (Sigma-Aldrich) was added. The plates were shaken for 10 min to thoroughly dissolve the formazan. The optical density (OD) at 490 nm was measured using an iMark microplate reader (Bio-Rad, Hercules, CA).

Colony formation assay

The cells after transfection or insulin treatment were used for colony formation assay. Briefly, single-cell suspensions of 200 cells were seeded in culture dishes (60 mm in diameter) containing the DMEM/F-12 medium supplemented with 10% FBS. After 2-week incubation in a humidified atmosphere with 5% CO₂ at 37°C, the medium was removed and the cells in dishes were washed twice in PBS. Methanol was added to fix the cells for 15 min, after which the cells were stained in Giemsa (HarveyBio, Beijing, China) for 20 min, washed, and air-dried. The colony number was counted and colony formation rate was calculated as (colony formation number/200) \times 100%.

Cell cycle assay

Single-cell suspension was prepared for the transfected cells and control groups at 24 h after transfection, and cell cycle was detected using Cell Cycle and Apoptosis Analysis Kit (Beyotime, Shanghai, China) according to the manufacturer's instructions. Briefly, the cells were fixed in ice-cold 70% ethanol at 4°C overnight, washed with PBS, and collected. Then, 500 μ L of new-made propidium iodide solution was added to cells for 30-min incubation in the dark at 37°C, after which the red fluorescence was detected at 488 nm using a flow cytometer (BD Biosciences, San Jose, CA) and analyzed with ModFit Lt (Verity Software House).

qRT-PCR

Tissue samples and cells at 24 h after transfection were collected and lysed in TRIzol (Invitrogen) or RNAiso for Small RNA (TaKaRa, Dalian, China) according to the manufacturer's instructions for total RNAs or miRNAs extraction. The complementary DNAs (cDNAs) were synthesized with total RNAs or miRNAs and the reverse transcription primer for miR-483-3p.2 (5'-CTC AAC TGG TGT CGT GGA GTC GGC AAT TCA GTT GAG AGG AGT GA-3') under the catalysis of PrimeScript Reverse Transcriptase (TaKaRa). qRT-PCR was performed on QuantStudio 6 Flex Realtime PCR system (Applied Biosystems, Carlsbad, CA) to detect the expression of hsa-miR-483-3p.2 (Fw: 5'-ACA CTC CAG CTG GGT CCA ACA TTG TCT TTA G-3' and Rv: 5'-TGG TGT CGT GGA GTC G-3'), *IGF1* (Fw: 5'-GCT CTT CAG TTC GTG TGT GG-3' and Rv: 5'-CGC AAT ACA TGT CCA GCC TC-3'), *CCNB1* (Fw: 5'-TAC CTA TGC TGG TGC CAG TG-3' and Rv: 5'-CAG ATG TTT CCA TTG GGC TT-3'), *CCND1* (Fw: 5'-CCT GTC CTA CTA CCG CCT CA-3' and Rv: 5'-TCC TCC TCT TCC TCC TC-3') and *CDK2* (Fw: 5'-CCT CCT GGG CTG CAA ATA-3' and Rv: 5'-CAG AAT CTC CAG

GGA ATA GGG-3'). Data were analyzed with 2^{- $\Delta\Delta$ CT} method compared to the control groups after standardized by GAPDH (Fw: 5'-GAA GGT GAA GGT CGG AGT C-3' and Rv: 5'-GAA GAT GGT GAT GGG ATT G-3').

Western blot

Total protein of cells at 24 h after transfection was extracted using RIPA lysis buffer (Beyotime, Shanghai, China) and separated on sodium dodecyl sulfate-polyacrylamide gel electrophoresis, after which they were transferred to a polyvinylidene fluoride membrane. The membrane was blocked in 5% skim milk for 2 h at room temperature and incubated in specific antibodies for IGF1 (ab9572), cyclin B1 (CCNB1, ab72), cyclin D1 (CCND1, ab16663) or cyclin-dependent kinase 2 (CDK2, ab32147, Abcam, Cambridge, UK) at 4°C overnight. GAPDH (ab181602) was detected as an internal reference. Then the membrane was washed in PBS and incubated in horseradish peroxidase-conjugated secondary antibodies for 1 h at room temperature, and then the signals were developed by EasyBlot ECL Kit (Sangon Biotech, Shanghai, China). The density of bands was compared to control groups after being standardized with GAPDH.

Statistical analysis

Data were analyzed using SPSS 20. For the analysis of endocrine tests, results were indicated as the mean \pm standard error of mean (SEM). The *t* test was used to test the significant difference in AGE, FSH, LH, PRL, E₂, and Glu between control and PCOS patients. The χ^2 test was performed to analyze the constituent ratio differences in BMI, T and INS between the 2 groups. All the other experiments were repeated 5 times and results are represented as the mean \pm standard deviation. The data were analyzed with the *F* test for analysis of variance and the *t* test for statistical significance. Differences between groups were considered significant if *P* < 0.05.

Results

miR-483 is down-regulated in PCOS tissues and it inhibits KGN cell proliferation

Endocrine tests in 20 PCOS patients and 20 non-PCOS individuals showed that BMI and endocrine levels possessed marked differences between the 2 groups (Table 1). The number of overweight individuals was significantly greater in the PCOS group (*P* < 0.01) and the PCOS patients had a significantly lower FSH level and significantly higher LH, PRL, E₂, and Glu levels than the control group (*P* < 0.05). A higher percentage of hyperandrogenism or hyperinsulinism was found in PCOS patients compared to controls (*P* < 0.05 and *P* < 0.01). These results

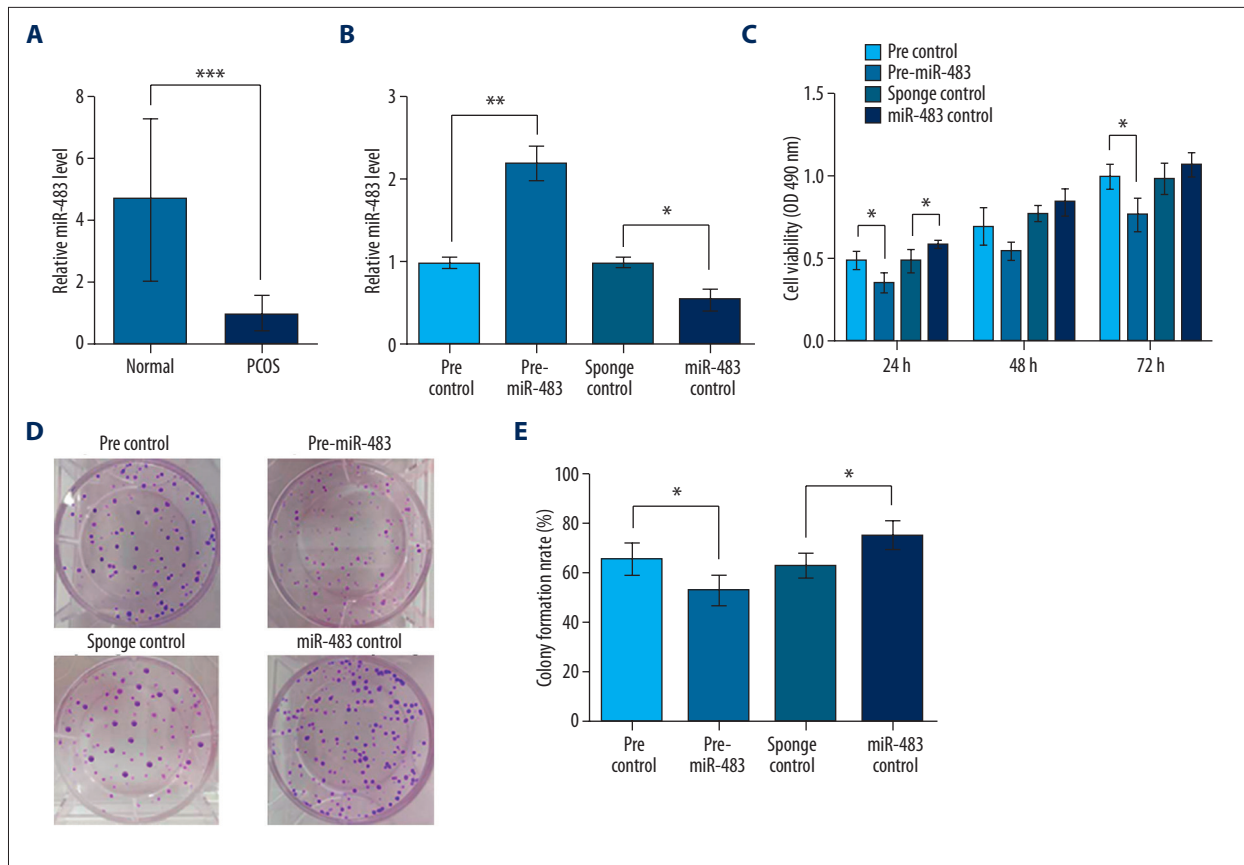


Figure 1. miR-483 is down-regulated in ovary cortex of PCOS patients and inhibits KGN cell viability and proliferation. pre-miR-483, KGN cells transfected with pre-miR-483. miR-483 sponge, KGN cells transfected with miR-483 sponge. pre/sponge control, KGN cells transfected with the corresponding blank vector as a control. (A) miR-483 expression in lesion and the adjacent normal ovary cortex from 20 PCOS patients as detected by qRT-PCR. (B) miR-483 expression was successfully altered by transfecting pre-miR-483 or miR-483 sponge in KGN cells. (C) Cell viability detected by MTT method at 24, 48, and 72 h after transfection. (D) Pictures of colony formation influenced by miR-483. (E) Colony formation rate calculated from colony formation assay. * $P < 0.05$. ** $P < 0.01$. *** $P < 0.001$. PCOS, polycystic ovarian syndrome.

indicate that the PCOS patients were more likely to be overweight and to have abnormal endocrine levels, which is consistent with the popular opinion that PCOS patients usually have hyperandrogenism, hyperinsulinism, and insulin resistance.

miR-483 was detected by qRT-PCR in lesions and the adjacent normal ovarian cortex tissues in the 20 PCOS patients (Figure 1A). Results showed a significantly lower miR-483 level in lesions than in normal tissues ($P < 0.001$), indicating that miR-483 was down-regulated in ovary cortex lesions of PCOS patients.

We then altered the expression of miR-483 by transfection in KGN cells and tested their validity (Figure 1B). These transfected cells were used for cell viability and colony formation assays. Cell viability assay showed that miR-483 overexpression led to the inhibition of cell viability, especially at 24 and 72 h after transfection ($P < 0.05$, Figure 1C). Correspondingly,

miR-483 knockdown promoted KGN cell viability compared to sponge control. Colony formation experiments showed similar changing patterns in which miR-483 overexpression decreased, and its knockdown increased, the colony number and formation rate ($P < 0.05$, Figure 1D, 1E). Taken together, these results suggest that miR-483 is capable of inhibiting KGN cell proliferation.

Given the suppressive role of miR-483 in KGN cell proliferation, the effect of miR-483 on KGN cell cycle was further analyzed by flow cytometry (Figure 2A). miR-483 overexpression increased cells in S and G2/M stages and decreased cells in G0/G1 stage, with significant changes detected in G1/G0 and S stages (Figure 2B). These results suggest that miR-483 might induce S or G2/M arrest in KGN cells. Then, we detected the mRNA and protein expression change of cell cycle factors CCNB1, CCND1, and CDK2 using qRT-PCR and Western blot. Results showed that the mRNA levels of the 3 factors

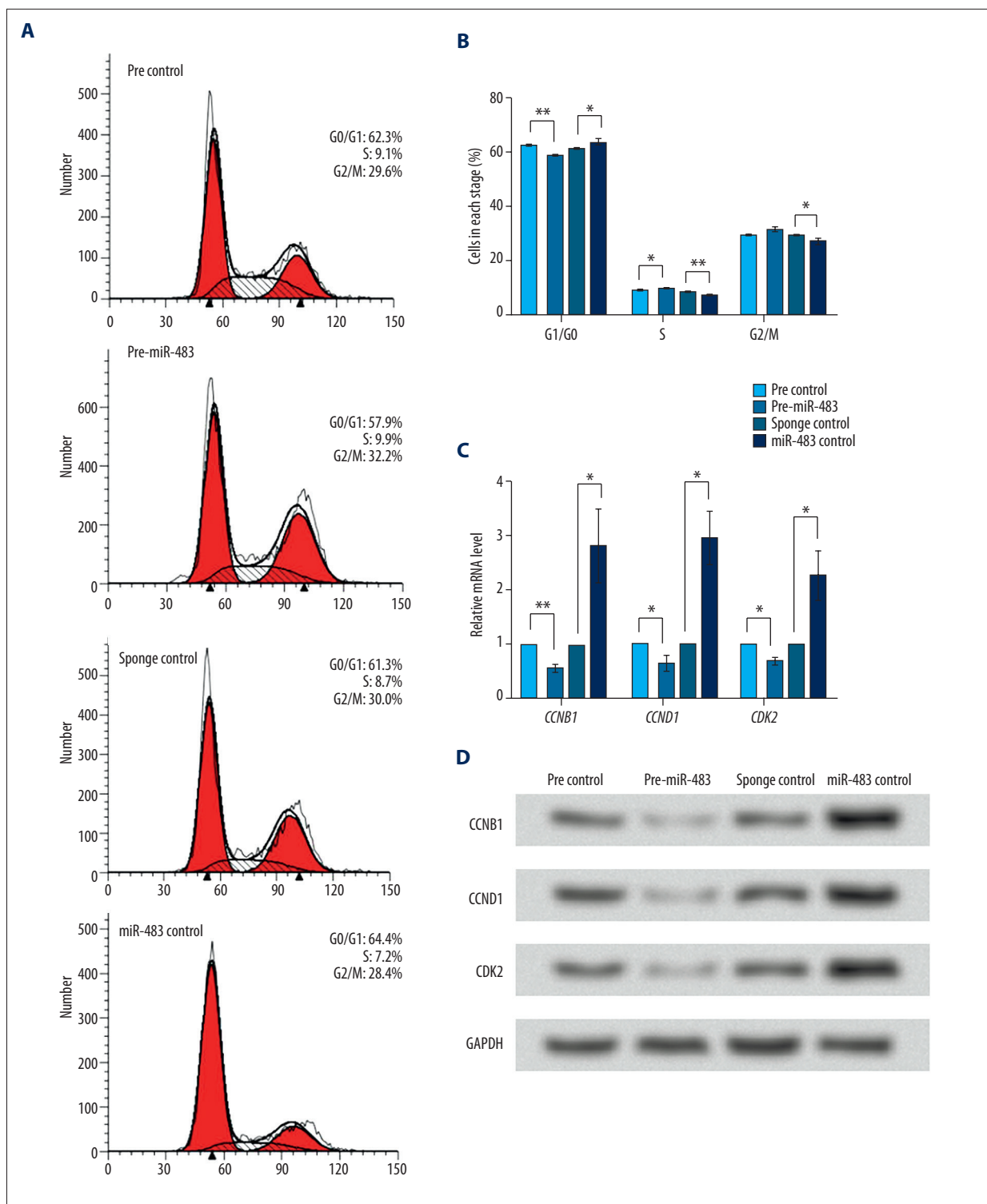


Figure 2. miR-483 induces cell cycle arrest in KGN cells. pre-miR-483, KGN cells transfected with pre-miR-483. miR-483 sponge, KGN cells transfected with miR-483 sponge. pre/sponge control, KGN cells transfected with the corresponding blank vector as a control. **(A)** Cell cycle analyzed by flow cytometry at 24 h after transfection. **(B)** Average cell percent in G1/G0, S, and G2/M stages. **(C)** mRNA levels of cell cycle factors *CCNB1*, *CCND1*, and *CDK2* detected by qRT-PCR with *GAPDH* as an internal reference. **(D)** Protein levels of *CCNB1*, *CCND1* and *CDK2* detected by Western blot with *GAPDH* as an internal reference. * $P < 0.05$. ** $P < 0.01$. *CCNB1* – cyclin B1. *CCND1* – cyclin D1. *CDK2* – cyclin-dependent kinase 2.

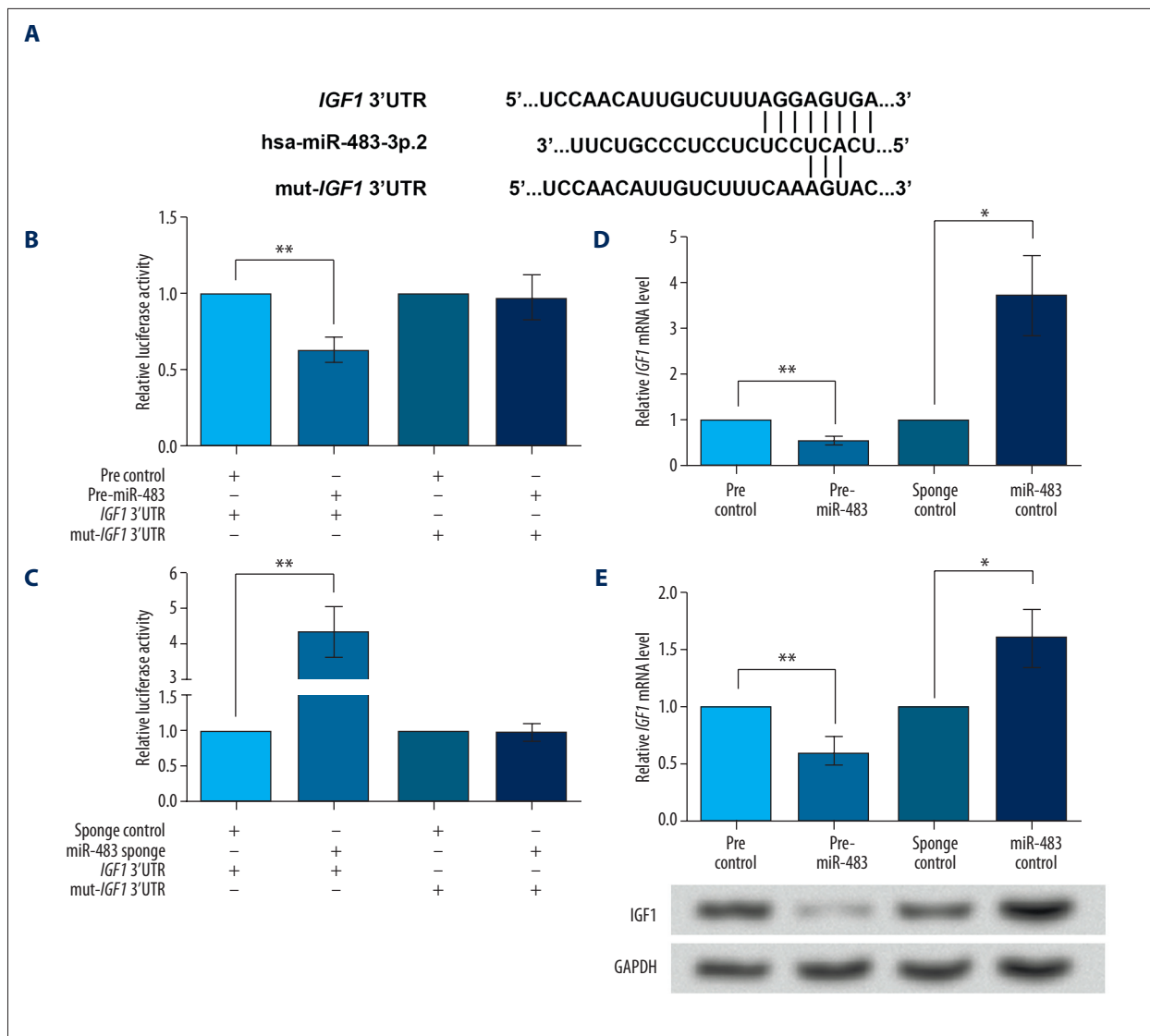


Figure 3. IGF1 is directly inhibited by miR-483. pre-miR-483, KGN cells transfected with pre-miR-483. miR-483 sponge, KGN cells transfected with miR-483 sponge. pre/sponge control, KGN cells transfected with the corresponding blank vector as a control. **(A)** The sequence AGGAGUGA in *IGF1* 3'UTR is predicted to be the binding site of miR-483. Five bases in the binding site are mutated to construct mut-*IGF1* 3'UTR. **(B)** Luciferase reporter assay shows that the activity of wildtype *IGF1* 3'UTR, but not mut-*IGF1* 3'UTR, can be inhibited by miR-483 overexpression compared to the control. **(C)** Luciferase reporter assay shows that the activity of wildtype *IGF1* 3'UTR, but not mut-*IGF1* 3'UTR, can be up-regulated by miR-483 sponge compared to sponge control. **(D)** *IGF1* mRNA expression was inhibited by miR-483 overexpression and promoted by miR-483 sponge, as shown by qRT-PCR. **(E)** IGF1 protein level was inhibited by miR-483 overexpression and promoted by miR-483 sponge, as shown by Western blot. GAPDH is used as an internal reference. * $P < 0.05$. ** $P < 0.01$. IGF1, insulin-like growth factor1. CCNB1 – cyclin B1. CCND1 – cyclin D1. CDK2 – cyclin-dependent kinase 2.

were decreased by miR-483 overexpression and increased by miR-483 knockdown ($P < 0.01$ or $P < 0.05$, Figure 2C). Their protein levels showed a similar changing pattern (Figure 2D). Therefore, we speculate that miR-483 might affect the expression of these cell cycle factors, which was associated with miR-483-induced cell cycle arrest.

IGF1 is a direct target of miR-483

As found in the endocrine tests, PCOS patients were prone to have higher insulin levels than non-PCOS women. Therefore, in this study we tried to analyze the relationship of miR-483 with insulin level. *IGF1* mRNA was predicted to be a target of miR-483 by the online database TargetScanHuman 7.0 (www.targets.org), with the sequence AGGAGUGA in its 3'UTR

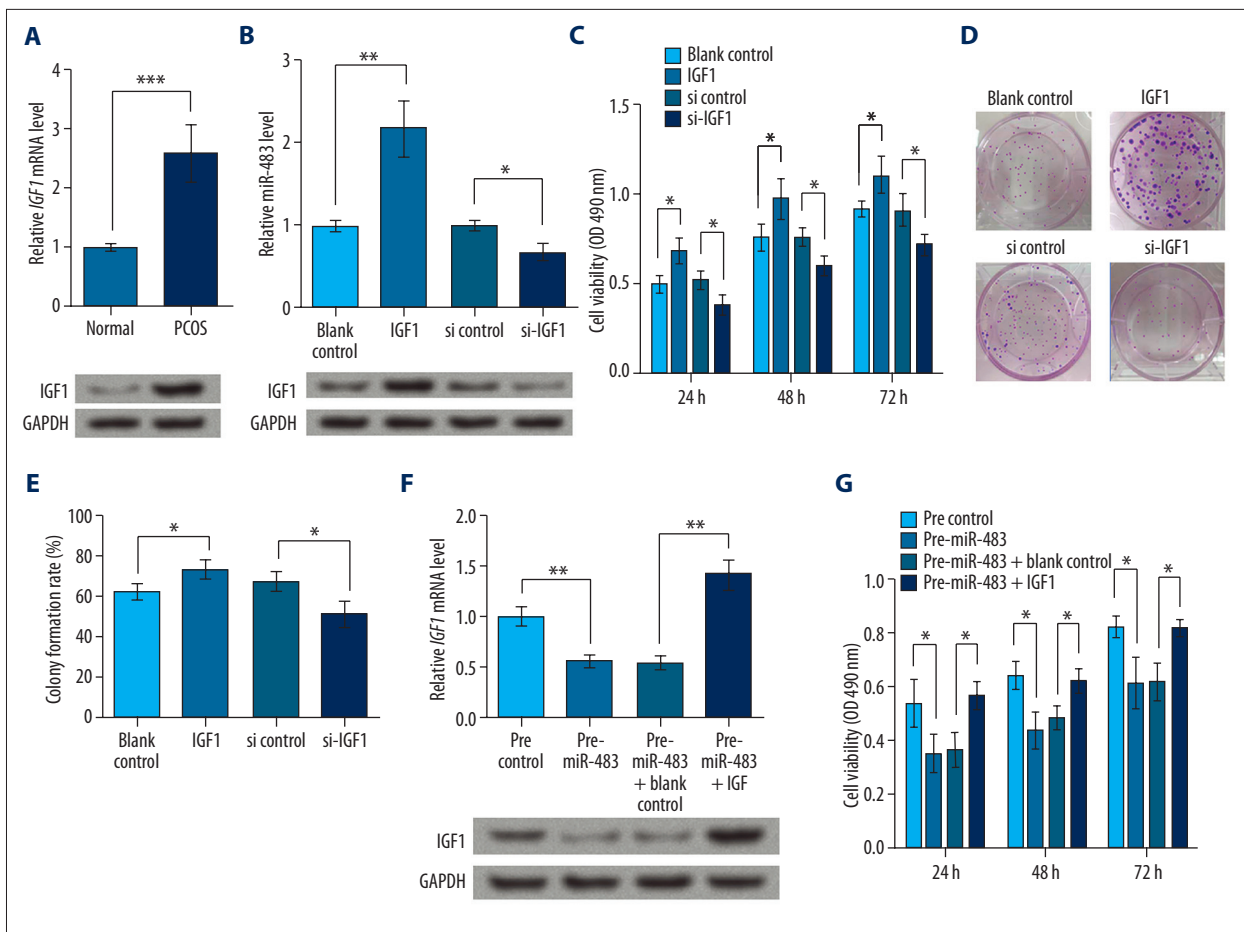


Figure 4. IGF1 promotes cell viability and proliferation in KGN cells. IGF1, KGN cells transfected with IGF1 overexpression vector. si-IGF1, KGN cells transfected with IGF1-specific siRNA. blank/si control, KGN cells transfection with the corresponding blank vectors as control groups. **(A)** IGF1 mRNA and protein expression was elevated in lesion ovary cortex of PCOS patients. **(B)** IGF1 mRNA and protein expression was altered by its overexpression vector or siRNA. **(C)** MTT assay shows KGN cell viability at 24, 48, and 72 h after transfection. **(D)** Pictures of colony formation. **(E)** Colony formation rate based on repeated colony formation assay experiment. **(F)** IGF1 expression in cells overexpressing miR-483 and IGF1 at the same time. **(G)** IGF1 overexpression in KGN cells transfected with miR-483 reverses miR-483-inhibited cell viability. * $P < 0.05$. ** $P < 0.01$. *** $P < 0.001$. IGF1 – insulin-like growth factor 1. PCOS – polycystic ovarian syndrome.

being the predicted binding site (Figure 3A). Therefore, dual-luciferase reporter assay was performed on the wildtype and mutant *IGF1* 3'UTR. miR-483 overexpression inhibited the activity of wildtype *IGF1* 3'UTR ($P < 0.01$, Figure 3B), but the activity of mutant *IGF1* 3'UTR was not altered. Similar results were found when miR-483 was inhibited ($P < 0.05$, Figure 3C), which supported that miR-483 could regulate IGF1 expression by acting on the binding site in *IGF1* 3'UTR. Indeed, miR-483 overexpression significantly inhibited *IGF1* mRNA expression ($P < 0.01$, Figure 3D) and its knockdown promoted *IGF1* mRNA level ($P < 0.05$). The IGF1 protein level exhibited similar changes ($P < 0.05$, Figure 3E). Taken together, these data suggest that miR-483 can directly bind to and inhibit IGF1 in KGN cells.

We next examined whether IGF1 was involved in the miR-483-regulated KGN proliferation. In the ovarian cortex of PCOS patients, *IGF1* mRNA level was significantly higher than in normal ovarian cortex ($P < 0.001$), and its protein expression was also elevated (Figure 4A). IGF1 was overexpressed and knocked down by transfection with its overexpression vector or specific siRNA, and the desired effects were acquired (Figure 4B). MTT assay showed that IGF1 overexpression could significantly up-regulate KGN cell viability and that its knockdown inhibited cell viability, with significant differences observed at 24, 48, and 72 h after transfection ($P < 0.05$, Figure 4C). Similarly, the colony formation rate of cells overexpressing IGF1 was increased compared to the controls, and that of cells with IGF1 knockdown was decreased ($P < 0.05$, Figure 4D, 4E). When overexpressing IGF1 in cells with elevated miR-483 (Figure 4F), IGF1

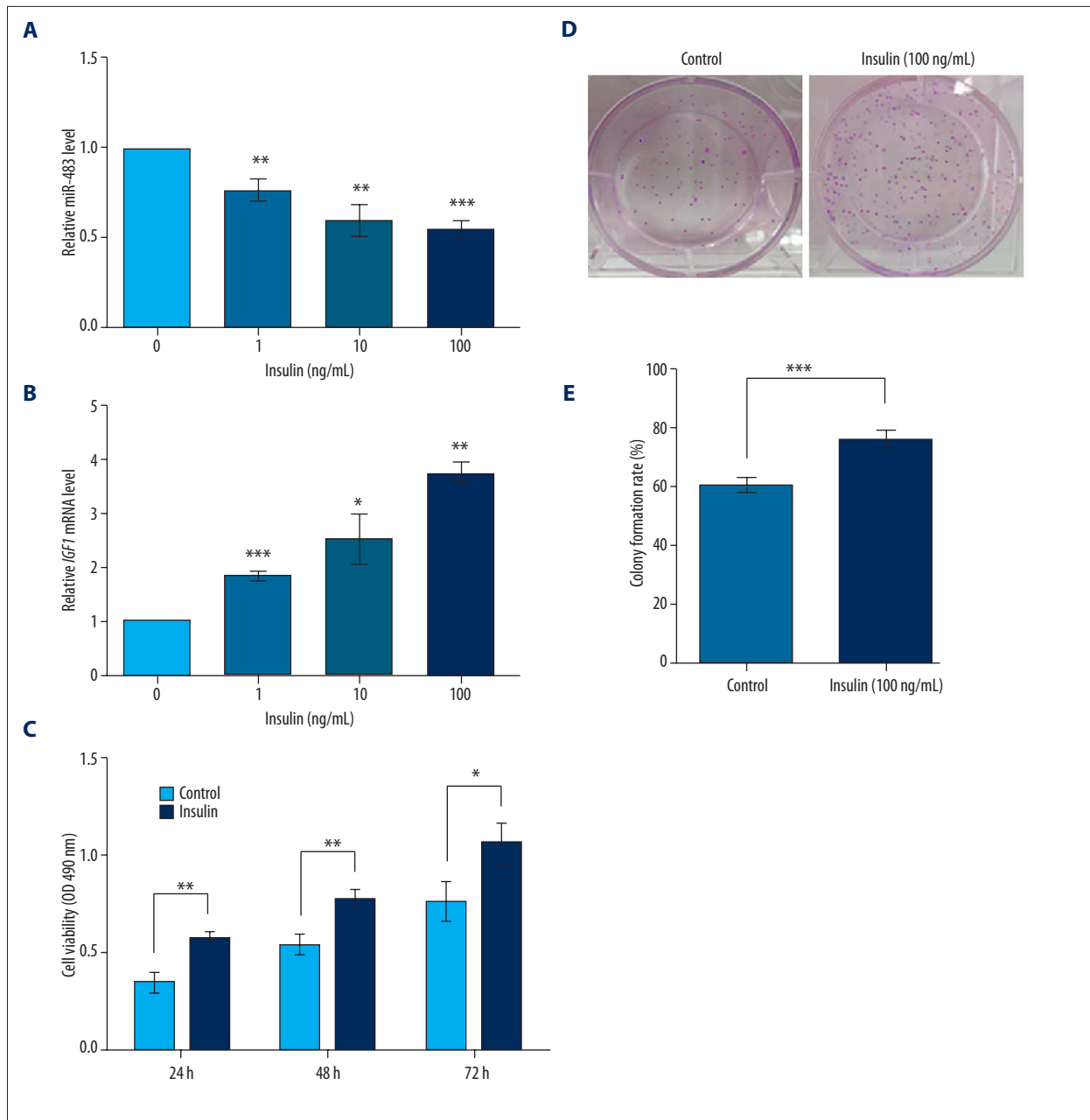


Figure 5. Insulin inhibits miR-483 and promotes IGF1 and KGN cell proliferation. **(A)** The miR-483 levels detected by qRT-PCR in cells treated with 0, 1, 10, and 100 ng/mL insulin for 48 h. **(B)** The *IGF1* mRNA levels detected by qRT-PCR in cells treated with 0, 1, 10, and 100 ng/mL insulin for 48 h. **(C)** Insulin (100 ng/mL) promotes KGN cell viability compared to the untreated cells (control). Cell viability was detected with MTT method after 24, 48, or 72 h of insulin treatment. **(D)** Pictures of colony formation assay. **(E)** Colony formation rate was increased by insulin (100 ng/mL) detected by colony formation assay after 48 h of insulin treatment. * $P < 0.05$. ** $P < 0.01$. *** $P < 0.001$. IGF1, insulin-like growth factor 1.

overexpression reversed the inhibited cell viability induced by miR-483 ($P < 0.05$, Figure 4G). These results show that IGF1 has functions opposite to miR-483, promoting cell viability and proliferation in KGN cells, which might suggest its association with the roles of miR-483 in KGN cells.

Insulin inhibits miR-483 and promotes KGN cell proliferation

Next, we analyzed the influence of insulin on miR-483 and IGF1 in KGN cells. The cells were treated with insulin of different concentrations (0, 1, 10, and 100 ng/mL) and miR-483 and *IGF1*

mRNA levels were detected by qRT-PCR. Results showed that miR-483 was suppressed and *IGF1* mRNA was induced by insulin, both in a dose-dependent pattern ($P < 0.05$, Figure 5A, 5B). Further, we detected cell viability and colony formation rate in KGN cells treated with 0 or 100 ng/mL insulin, and results showed that insulin treatment significantly promoted KGN cell viability at 24, 48, and 72 h after treatment ($P < 0.05$, Figure 5C). Also, insulin treatment increased the colony formation rate of KGN cells compared to untreated cells ($P < 0.01$, Figure 5D, 5E). These data indicate that insulin inhibited miR-483 and promoted IGF1, which is consistent with its roles in promoting KGN cell viability and proliferation.

Discussion

In this study, miR-483 was found to be down-regulated in the ovarian cortex lesion of PCOS patients. In KGN cells, miR-483 overexpression leads to inhibited cell viability and proliferation. Dual-luciferase reporter assay shows *IGF1* is a direct target for miR-483 and promotes KGN cell proliferation. Insulin treatment in KGN cells inhibits miR-483, promotes IGF1, and induces cell proliferation.

CCNB1, CCND1, and CDK2 are 3 important cell cycle regulators associated with cell cycle arrest, as reported in previous studies. CCNB1 elevation is capable of promoting ATP production to facilitate G2/M transition and cell cycle progression [21]. As a partner of A- and E-type cyclins, CDK2 functions in S and G2 phases and activates G2/M checkpoint [22]. Restrained expression of CCND1 results in G2/M arrest [23]; therefore, CCND1 is also a key intervention point in the cell cycle. In this study, the expression of these factors were changed by miR-483 and accompanied with S or G2/M arrest by flow cytometry, showing that miR-483 can regulate these cell cycle factors, induce cell cycle arrest, and further contribute to the inhibited proliferation of KGN cells.

IGF1 is an insulin-linked peptide involved in the development of insulin resistance-related metabolic disorders such as obesity and type 2 diabetes [24]. Circulating IGF1 concentration is positively correlated with increased risk of prostate cancer [25]. In the serum of PCOS patients, IGF1 level is markedly up-regulated compared to that in normal persons [26]. In this study, IGF1 was elevated in the ovary cortex lesions of PCOS patients. IGF1 promoted KGN cell viability and proliferation, and reversed the inhibited cell viability by miR-483. Together with the direct inhibition of IGF1 by miR-483, we speculate that IGF1 is a key modulator in the miR-483-suppressed KGN cell proliferation.

miR-483-5p has been revealed to be down-regulated in the cumulus cells of PCOS patients [19], which may imply the suppressed functions of miR-483-5p in PCOS development. miR-483-3p inhibits keratinocyte migration and proliferation during wound closure via directly targeting kinase *MK2*, cell proliferation marker *MKI67*, and transcription factor *YAP1* [27], and induces cell cycle arrest by decreasing CCND-CDK4/6 assembly [28]. In squamous cell carcinoma, miR-483 targets anti-apoptotic genes like *API5*, *BIRC5*, and *RAN* to exert tumor suppressor activities [29]. Similarly, in this study, miR-483-3p was confirmed to inhibit KGN cell proliferation and arrest cell cycle, possibly via suppressing IGF1, implying the potential utility of miR-483 as a biomarker and therapeutic alternative for diagnosing and treating PCOS.

PCOS is associated with several metabolic disorders, including insulin resistance, unbalanced hormone levels, obesity, and diabetes [30]. Insulin resistance is prone to induce hyperandrogenism, and therapeutic strategies for insulin resistance in PCOS patients may alleviate obesity and hyperandrogenism at the same time [31–33]. In the endocrine tests of PCOS patients, we observed elevated blood glucose level, insulin level, androgen level, and a higher BMI, implying a higher risk of insulin resistance in these PCOS patients, which might contribute to the progression of PCOS. In the circumstance of insulin resistance, high insulin level can induce cell proliferation, as reported in type I endometrial carcinoma and pancreatic beta cells [34,35]. In line with former studies, insulin treatment in KGN cells could also promote cell viability and proliferation, inhibit miR-483, and promote IGF1, so it is possible that the effects of insulin on KGN cell proliferation involve the regulation of miR-483 and its target, IGF1. Based on these findings, miR-483 is likely to be a potent modulator of insulin resistance in PCOS patients, but further studies are needed.

Conclusions

miR-483 is down-regulated in the ovary cortex of PCOS patients. Overexpression of miR-483 suppresses KGN cell viability and proliferation, and induces cell cycle arrest. The function of miR-483 on KGN proliferation is possibly executed via regulating IGF1, a factor promoting KGN cell proliferation. Therefore, miR-483 is a potential therapeutic strategy for diagnosing and treating PCOS.

Conflicts of interest

There are no conflicts of interest.

References:

1. Trivax B, Azziz R: Diagnosis of polycystic ovary syndrome. *Clin Obstet Gynecol*, 2007; 50: 168–77
2. Pieta W, Wilczynska A, Radowski S: Hydrolaparoscopy – as an alternative method after a failure of the pharmacological therapy for PCOS induced infertility. *Gynecology & Obstetrics* 2014; 04: 222
3. Misso ML, Teede HJ, Hart R et al: Status of clomiphene citrate and metformin for infertility in PCOS. *Trends Endocrinol Metab*, 2012; 23: 533–43
4. Moran LJ, Hutchison SK, Norman RJ, Teede HJ: Lifestyle changes in women with polycystic ovary syndrome. *Cochrane Database Syst Rev*, 2011; 2011: CD007506
5. Chang RJ, Cook-Andersen H: Disordered follicle development. *Mol Cell Endocrinol*, 2013; 373: 51–60
6. Lewandowski KC, Cajdler-tuba A, Salata I et al: The utility of the gonadotrophin releasing hormone (GnRH) test in the diagnosis of polycystic ovary syndrome (PCOS). *Endokrynol Pol*, 2011; 62: 120–28
7. Azziz R, Carmina E, Dewailly D et al: Positions statement: Criteria for defining polycystic ovary syndrome as a predominantly hyperandrogenic syndrome: An Androgen Excess Society guideline. *J Clin Endocrinol Metab*, 2006; 91: 4237–45
8. Ehrmann DA, Barnes RB, Rosenfield RL: Polycystic ovary syndrome as a form of functional ovarian hyperandrogenism due to dysregulation of androgen secretion. *Endocr Rev*, 2013; 16: 322–53
9. Apparao KB, Lovely LP, Gui Y et al: Elevated endometrial androgen receptor expression in women with polycystic ovarian syndrome. *Biol Reprod*, 2002; 66: 297–304
10. Gambineri A, Pelusi C, Vicennati V et al: Obesity and the polycystic ovary syndrome. *Int J Obes Relat Metab Disord*, 2002; 26(7): 883–96
11. Diamanti-Kandarakis E, Dunaif A: Insulin resistance and the polycystic ovary syndrome revisited: An update on mechanisms and implications. *Endocr Rev*, 2012; 33: 981–1030
12. Holte J, Bergh T, Berne C et al: Enhanced early insulin response to glucose in relation to insulin resistance in women with polycystic ovary syndrome and normal glucose tolerance. *J Clin Endocrinol Metab*, 1994; 78: 1052–58
13. Çakir E, Topaloğlu O, Çolak Bozkurt N et al: Insulin-like growth factor 1, liver enzymes, and insulin resistance in patients with PCOS and hirsutism. *Turk J Med Sci*, 2014; 44: 781–86
14. Thierry van Dessel HJ, Lee PD, Faessen G et al: Elevated serum levels of free insulin-like growth factor I in polycystic ovary syndrome. *J Clin Endocrinol Metab*, 1999; 84: 3030–35
15. Premoli AC, Santana LF, Ferriani RA et al: Growth hormone secretion and insulin-like growth factor-1 are related to hyperandrogenism in nonobese patients with polycystic ovary syndrome. *Fertil Steril*, 2005; 83: 1852–55
16. Jiang L, Huang J, Li L et al: MicroRNA-93 promotes ovarian granulosa cells proliferation through targeting CDKN1A in polycystic ovarian syndrome. *J Clin Endocrinol Metab*, 2015; 100: E729–38
17. Sathyapalan T, David R, Gooderham NJ, Atkin SL: Increased expression of circulating miRNA-93 in women with polycystic ovary syndrome may represent a novel, non-invasive biomarker for diagnosis. *Sci Rep*, 2015; 5: 16890
18. Chen YH, Heneidi S, Lee JM et al: miRNA-93 inhibits GLUT4 and is overexpressed in adipose tissue of polycystic ovary syndrome patients and women with insulin resistance. *Diabetes*, 2013; 62: 2278–86
19. Shi L, Liu S, Zhao W, Shi J: miR-483-5p and miR-486-5p are down-regulated in cumulus cells of metaphase II oocytes from women with polycystic ovary syndrome. *Reprod Biomed Online*, 2015; 31: 565–72
20. Pellicano M, Zullo F, Cappiello F et al: Minilaparoscopic ovarian biopsy performed under conscious sedation in women with premature ovarian failure. *J Reprod Med*, 2000; 45: 817–22
21. Wang Z, Fan M, Candas D et al: Cyclin B1/Cdk1 coordinates mitochondrial respiration for cell-cycle G2/M progression. *Dev Cell*, 2014; 29: 217–32
22. Chung JH, Bunz F: Cdk2 is required for p53-independent G2/M checkpoint control. *PLoS Genet*, 2010; 6: e1000863
23. Khandelwal P, Padala MK, Cox J, Guntaka RV: The N-terminal domain of y-box binding protein-1 induces cell cycle arrest in G2/m phase by binding to cyclin d1. *Int J Cell Biol*, 2009; 2009: 243532
24. Djiogoe S, Nwabo Kamdje AH, Vecchio L et al: Insulin resistance and cancer: The role of insulin and IGFs. *Endocr Relat Cancer*, 2013; 20: R1–17
25. Price AJ, Allen NE, Appleby PN et al: Insulin-like growth factor-I concentration and risk of prostate cancer: Results from the European Prospective Investigation into Cancer and Nutrition. *Cancer Epidemiol Biomarkers Prev*, 2012; 21: 1531–41
26. Xu SY, Zhao SP, Ma DH et al: The changes of serum TNF-alpha and IGF-1 and their significance in patients with polycystic ovarian syndrome. *Acta Academiae Medicinae Qingdao Universitatis*, 2010; 46: 45–48 [in Chinese]
27. Bertero T, Gastaldi C, Bourget-Ponzio I et al: miR-483-3p controls proliferation in wounded epithelial cells. *FASEB J*, 2011; 25: 3092–105
28. Bertero T, Gastaldi C, Bourget-Ponzio I et al: CDC25A targeting by miR-483-3p decreases CCND-CDK4/6 assembly and contributes to cell cycle arrest. *Cell Death Differ*, 2013; 20: 800–11
29. Bertero T, Bourget-Ponzio I, Puissant A et al: Tumor suppressor function of miR-483-3p on squamous cell carcinomas due to its pro-apoptotic properties. *Cell Cycle*, 2013; 12: 2183–93
30. San Millan JL, Corton M, Villuendas G et al: Association of the polycystic ovary syndrome with genomic variants related to insulin resistance, type 2 diabetes mellitus, and obesity. *J Clin Endocrinol Metab*, 2004; 89: 2640–46
31. Brettenthaler N, De Geyter C, Huber PR, Keller U: Effect of the insulin sensitizer pioglitazone on insulin resistance, hyperandrogenism, and ovulatory dysfunction in women with polycystic ovary syndrome. *J Clin Endocrinol Metab*, 2004; 89: 3835–40
32. Diamanti-Kandarakis E, Kouli C, Tsianateli T, Bergiele A: Therapeutic effects of metformin on insulin resistance and hyperandrogenism in polycystic ovary syndrome. *Eur J Endocrinol*, 1998; 138: 269–74
33. Selimoglu H, Duran C, Kiyici S et al: The effect of vitamin D replacement therapy on insulin resistance and androgen levels in women with polycystic ovary syndrome. *J Endocrinol Invest*, 2010; 33: 234–38
34. Li X, Shao R: PCOS and obesity: insulin resistance might be a common etiology for the development of type I endometrial carcinoma. *Am J Cancer Res*, 2014; 4: 73–79
35. Ogino J, Sakurai K, Yoshiwara K et al: Insulin resistance and increased pancreatic beta-cell proliferation in mice expressing a mutant insulin receptor (P1195L). *J Endocrinol*, 2006; 190: 739–47